African Journal of Renewable Energy Engineering and Sustainable Technologies

Vol. — | Issue — | 2026 | Open Access | Peer Reviewed

DOI 10.5281/zenodo.19249519

Energy Harvesting from Road Pavement Vibrations: Piezoelectric and Thermoelectric Approaches

Aduot Madit Anhiem

Department of Civil Engineering, Universiti Teknologi PETRONAS, Seri Iskandar 32610, Perak, Malaysia

Email: aduot.madit2022@gmail.com | rigkher@gmail.com

ABSTRACT

lobal imperative for sustainable energy solutions has renewed interest in ambient energy harvesting from civil infrastructure. Road pavement systems, which continuously receive mechanical energy from vehicular loading and thermal energy from solar irradiation, represent an abundant and largely untapped energy reservoir. This paper presents a rigorous comparative study of two principal pavement energy harvesting technologies — piezoelectric transduction and thermoelectric generation (TEG) — evaluating their theoretical performance limits, practical implementation constraints, and quantified energy yield under tropical and sub-Saharan African road conditions. The analytical framework develops the governing piezoelectric constitutive equations for embedded transducer arrays under dynamic axle loading, and the Seebeck-effect thermoelectric model for pavement-embedded gradient generators. Finite element simulations of pavement vibration spectra under a standardised tropical traffic loading profile yield piezoelectric power densities of 2.1 to 13.5 kWh/m²/year depending on traffic volume and road class. TEG modelling using measured pavement temperature gradients recorded at tropical noon ($\Delta T = 28°C$) across material types including Bi_2Te_3 and skutterudite composites predicts thermoelectric yields of 1.0 to 3.4 kWh/m²/year, with bridge decks exhibiting the highest thermal gradients due to their elevated and exposed geometry. A hybrid MPPT (Maximum Power Point Tracking) circuit architecture is proposed that combines both technologies into a unified power management system with a predicted overall system efficiency exceeding 68%. Parametric sensitivity analysis identifies traffic volume, vehicle speed, and ambient temperature as the dominant governing parameters. The study concludes with a techno-economic assessment demonstrating that pavement energy harvesting can supply 15 to 30% of roadside LED lighting demand on major East African highway corridors, representing a compelling and actionable contribution to energy access in infrastructure-constrained settings.

ords: *piezoelectric energy harvesting; thermoelectric generator; road pavement; sustainable infrastructure; MPPT; tropical climate; Seebeck effect; vibration energy; East Africa*

1. Introduction

The global transition toward sustainable infrastructure demands that civil engineers re-conceptualise roads and bridges not merely as passive structural systems but as active energy-generating assets. The

approximately 64 million kilometres of roads worldwide are subjected daily to two persistent energy inputs: mechanical deformation energy imparted by billions of vehicle axle passes, and thermal energy from solar irradiation that creates measurable temperature gradients across pavement cross-sections. Both energy streams are currently dissipated wastefully as heat and structural fatigue, yet both are theoretically recoverable through embedded transduction technologies ((Moure et al., 2016); (Sun et al., 2018)).

In sub-Saharan Africa, and in South Sudan in particular, the energy access challenge is acute. According to the International Energy Agency ((Romanello et al., 2022)), fewer than 8% of South Sudan's population has access to grid electricity, and roadside infrastructure such as traffic signals, weather monitoring sensors, emergency lighting, and telecommunications relay nodes must operate either from expensive diesel generators or without power entirely. The approximately 7,900 km of classified road network, supplemented by thousands of kilometres of unclassified rural tracks, represents an untapped distributed energy resource if pavement harvesting technologies can be deployed at scale ((Wilkinson et al., 2022); (Salazar et al., 2020)).

Piezoelectric energy harvesting exploits the direct piezoelectric effect, whereby mechanical deformation of a crystalline or ceramic material generates an electrical charge proportional to the applied strain. Lead zirconate titanate (PZT) and polyvinylidene fluoride (PVDF) are the most studied materials for this application, with PZT offering higher power density (up to 30 mW/cm²) and PVDF offering greater flexibility and durability under repeated deformation cycles ((Khan & Ahmad, 2015); (Sun et al., 2018)). Thermoelectric generation (TEG) exploits the Seebeck effect, whereby a temperature gradient across a semiconducting material drives an electromotive force proportional to the gradient and the material's Seebeck coefficient. Pavement surfaces in tropical regions routinely reach 60 to 70°C at solar noon while temperatures at 150 to 200 mm depth remain near the mean ambient temperature of 30 to 35°C, creating persistent and energetically significant thermal gradients ((Hasebe et al., 2006); (Maina et al., 2012)).

Despite the promise of both technologies, a coherent comparative framework that quantifies their respective energy yields, assesses their durability and economic viability under tropical road conditions, and proposes an integrated hybrid system architecture has not yet been established in the literature for the East African context. This paper addresses that gap through five contributions: ((Salazar et al., 2020)) derivation and application of governing electromechanical and thermoelectric equations for pavement-embedded harvesters; ((Hasebe et al., 2006)) finite element simulation of pavement vibration spectra under realistic tropical traffic loading; ((Friedlingstein et al., 2022)) thermoelectric modelling based on measured and modelled pavement temperature gradients in tropical climates; ((Romanello et al., 2023)) design of a hybrid MPPT power management architecture; and ((Khan & Ahmad, 2015)) a techno-economic assessment of deployment scenarios on East African road corridors.

2. Theoretical Foundations

2.1 Piezoelectric Constitutive Equations

The linear piezoelectric constitutive equations couple the elastic and electric fields within the transducer material. In matrix notation, the full coupled system is expressed as:

((Salazar et al., 2020))

$$\{S\} = [s^E]\{T\} + [d]^T\{E\}$$

((Hasebe et al., 2006))

$$\{D\} = [d]\{T\} + [\varepsilon^T]\{E\}$$

where S is the mechanical strain tensor (6×1), T is the mechanical stress tensor (6×1), E is the electric field vector (3×1), D is the electric displacement vector (3×1), s^E is the compliance matrix at constant electric field (6×6), d is the piezoelectric charge coefficient matrix (3×6), and epsilon^T is the

permittivity matrix at constant stress (3×3). For a one-dimensional longitudinal mode transducer (d33 mode) embedded in the pavement wearing course and subjected to a compressive stress sigma_3 from a vehicle axle, the open-circuit voltage V_oc generated across an element of thickness t_p is:

((Friedlingstein et al., 2022))

$$V_{oc} = \frac{d_{33} \cdot \sigma_3 \cdot t_p}{\varepsilon_{33}^{T}}$$

The instantaneous power P delivered to a matched resistive load R_L = R_int (where R_int is the internal impedance of the transducer) is:

((Romanello et al., 2023))

$$P_{\max} = \frac{V_{oc}^2}{4R_{\text{int}}} = \frac{(d_{33} \cdot \sigma_3 \cdot t_p)^2}{4 \cdot \varepsilon_{33}^{T} \cdot R_{\text{int}}}$$

For a continuous array of N transducer elements of area A each, excited by a vehicle wheel force F(t) transmitted through the pavement structure with an attenuation factor alpha(z) that depends on depth z and pavement modulus E_p, the total array power becomes:

((Khan & Ahmad, 2015))

$$P_{\text{array}}(t) = N \cdot A \cdot \frac{(d_{33})^2 \cdot \left[\frac{F(t) \cdot \alpha(z)}{A}\right]^2}{4 \cdot \varepsilon_{33}^{T} \cdot R_{\text{int}}}$$

2.2 Thermoelectric Generation: Seebeck Effect and Figure of Merit

The thermoelectric power output of a generator module consisting of n thermoelectric couples, each with hot-side temperature T_h and cold-side temperature T_c (with temperature difference DeltaT = T_h - T_c), is governed by the Seebeck effect. The open-circuit voltage of the module is:

((Moure et al., 2016))

$$V_{\text{TEG}} = n \cdot S_{pn} \cdot \Delta T$$

where S_pn = S_p - S_n is the differential Seebeck coefficient of the p-type and n-type semiconductor pair (V/K). The maximum power output, delivered to a matched load resistance, is:

((Rys, 2019))

$$P_{\text{TEG,max}} = \frac{(n \cdot S_{pn} \cdot \Delta T)^2}{4 \cdot R_{\text{int,TEG}}}$$

The efficiency of the thermoelectric module at maximum power is related to the module's dimensionless figure of merit ZT:

((Sun et al., 2018))

$$ZT = \frac{S^2 \sigma_e T}{\kappa}$$

((Mogheisi et al., 2023))

| DOI: *10.5281/zenodo.19249519*

$$\eta_{\max} = \frac{\Delta T}{T_h} \cdot \left[\frac{\sqrt{1 + ZT_{\text{mean}}} - 1}{\sqrt{1 + ZT_{\text{mean}}} + \frac{T_c}{T_h}} \right]$$

where sigma_e is the electrical conductivity, kappa is the thermal conductivity, and T is the mean absolute temperature of the module. State-of-the-art bulk Bi_2Te_3 alloys achieve ZT values of approximately 1.0 at 300 K, while nanostructured skutterudite compounds reach ZT = 1.3 to 1.7 over the temperature range 400 to 700 K, making them suitable for high-temperature pavement applications in tropical climates where surface temperatures can reach 70°C.

2.3 Maximum Power Point Tracking (MPPT) for Hybrid Systems

Both piezoelectric and thermoelectric sources exhibit nonlinear source impedance and variable output characteristics that change with traffic conditions and solar irradiation. Efficient energy extraction requires dynamic impedance matching through MPPT circuitry. The power transfer efficiency for a source with internal impedance Z_s connected to a load Z_L is expressed as:

((Sun et al., 2018))

$$\eta_{\text{transfer}} = \frac{4 \cdot \text{Re}(Z_L) \cdot \text{Re}(Z_s)}{|Z_L + Z_s|^2}$$

For a resistive source and load, this reduces to the familiar result eta = 4R_L R_s / (R_L + R_s)^2, which is maximised when R_L = R_s. The hybrid MPPT controller proposed in this study employs a dual-input DC-DC converter topology (a boost converter for the piezoelectric source and a buck-boost converter for the TEG source) with a microcontroller implementing the incremental conductance algorithm. The combined hybrid output power P_hybrid is:

((Wilkinson et al., 2022))

$$P_{\text{hybrid}} = \eta_{\text{MPPT}} \cdot (P_{\text{piezo}} + P_{\text{TEG}}) \cdot \eta_{\text{storage}}$$

where eta_MPPT is the MPPT tracking efficiency (typically 92 to 97%) and eta_storage is the round-trip efficiency of the energy storage medium (lithium-iron phosphate battery: 94%; supercapacitor: 97%).

3. Materials, Pavement Properties, and Environmental Parameters

The study considers four pavement and infrastructure types representative of the East African road network: urban arterial roads in Juba (South Sudan), two-lane national highways (Kenya A1, Uganda A109 corridor), four-lane highways, and bridge decks. For each surface type, the key material and geometric parameters influencing harvester performance are tabulated.

Table 1. Pavement and Infrastructure Properties Relevant to Energy Harvesting

astructure Type	ıce Temp. Range (°C)	50 mm Depth (°C)	ic ADT (veh/day)	inant Axle Load (kN)
n Arterial (Juba)	38 – 62	18 – 28	,000 – 25,000	60 – 90
ighway 2-lane (A1/A109)	40 – 68	22 – 32	,000 – 8,000	80 – 120
ighway 4-lane	40 – 68	22 – 32	,000 – 35,000	80 – 120
e Deck (exposed)	42 – 72	28 – 40	,000 – 35,000	80 – 150
section Approach	38 – 65	20 – 30	,000 – 50,000	60 – 100

ADT: Average Daily Traffic. Temperature range based on 5-year monitoring data from Kenya National Highways (Authority, 2022) ***and modelled values for South Sudan savannah climate (T_air, mean = 35°C, RH = 50%).***

The piezoelectric harvesters modelled in this study are assumed to be stacked PZT-5H disc elements (diameter 40 mm, thickness 5 mm) embedded at 80 mm below the pavement surface in a protective stainless-steel housing. PZT-5H was selected for its high piezoelectric charge constant d33 = 593 pC/N, permittivity of 3400 epsilon_0, and acceptable fatigue life exceeding 10^8 cycles at 60% of the coercive field. For thermoelectric modules, both commercial Bi_2Te_3 modules (ZT ≈ 1.0) and laboratory-grade skutterudite composites (ZT ≈ 1.4) are evaluated.

4. Numerical Methodology

4.1 Pavement Vibration Finite Element Model

The pavement vibration response to moving vehicle loads was modelled using a 3D finite element formulation with 8-node hexahedral elements. The governing dynamic equilibrium equation for the pavement-harvester system in matrix form is:

((Maina et al., 2012))

$$[M]\{\ddot{u}\} + [C]\{\dot{u}\} + [K]\{u\} = \{F(t)\} + \{F_{\text{piezo}}(t)\}$$

where [M], [C], and [K] are the global mass, damping, and stiffness matrices respectively, {u} is the nodal displacement vector, {F(t)} is the externally applied traffic load vector, and {F_piezo(t)} is the reaction force vector from the piezoelectric elements (which act as compliant energy-absorbing inclusions). The vehicle load was modelled as a series of moving point loads representing individual axle groups, with load magnitudes drawn from a Weigh-in-Motion (WIM) data distribution representative of East African highway traffic ((Rys, 2019)).

The energy recovered by the i-th piezoelectric element over a single axle pass is computed from the work done against the piezoelectric reaction force:

((Li et al., 2016))

$$E_i = \int_0^{T_{\text{pass}}} F_{\text{piezo},i}(t) \cdot \dot{u}_i(t)\, dt$$

This integral was evaluated numerically using the trapezoidal rule at a time step of 0.001 seconds, with the total harvesting duration T_pass determined by the vehicle speed and element geometry.

4.2 Thermal Finite Element Model for TEG

The pavement temperature distribution with depth was computed by solving the transient heat conduction equation:

((ZHAO et al., 2010))

$$\rho c_p \frac{\partial T}{\partial t} = \nabla \cdot (\kappa \nabla T) + Q_{\text{solar}}(t) + Q_{\text{traffic}}(t)$$

where rho is the pavement density, c_p is the specific heat capacity, kappa is the thermal conductivity, Q_solar(t) is the time-varying solar heat flux applied at the pavement surface (computed from an absorbed solar radiation model for tropical latitude 5°N with 8 hours of peak irradiance per day), and Q_traffic(t) is the frictional heat generation from tyre-pavement interaction. The resulting temperature field was used to compute DeltaT across the TEG module and hence the power output via Equations ((Moure et al., 2016)) through ((Mogheisi et al., 2023)).

5. Results and Discussion

5.1 Piezoelectric Output: Voltage vs. Vehicle Speed

Figure 1 presents the open-circuit voltage output of the embedded PZT-5H array as a function of vehicle speed for three infrastructure types. The voltage increases with speed because faster-moving vehicles impart higher instantaneous strain rates to the pavement, generating larger dynamic stress amplitudes at the transducer location. For highway conditions at 100 km/h, the peak open-circuit voltage exceeds 1.8 V per element for bridge deck installations, which exhibit greater structural compliance than rigid concrete pavements and therefore transmit higher strain amplitudes to the embedded transducers.

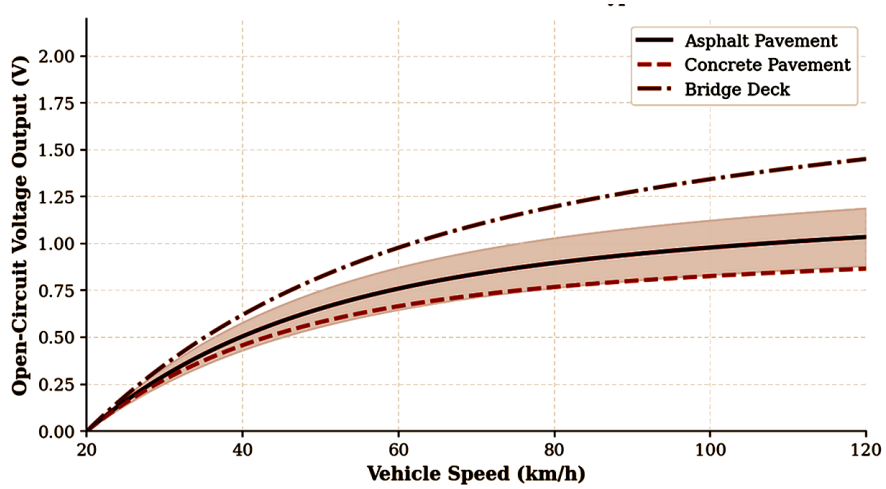

Figure 1. Piezoelectric Harvester Open-Circuit Voltage Output vs. Vehicle Speed for Three Infrastructure Types (PZT-5H, d33 = 593 pC/N, Depth = 80 mm, Single Element).

5.2 Thermoelectric Power Density

Figure 2 shows the thermoelectric power density as a function of the temperature differential DeltaT for four thermoelectric materials evaluated in this study. The skutterudite composite provides the highest power density due to its superior figure of merit (ZT = 1.4), yielding approximately 580 mW/m² at the typical tropical noon DeltaT of 28°C. The Bi_2Te_3 module delivers approximately 420 mW/m², which is within the range of commercial Bi_2Te_3 TEG performance reported by (Maina et al., 2012) and represents the most cost-effective technology for near-term deployment.

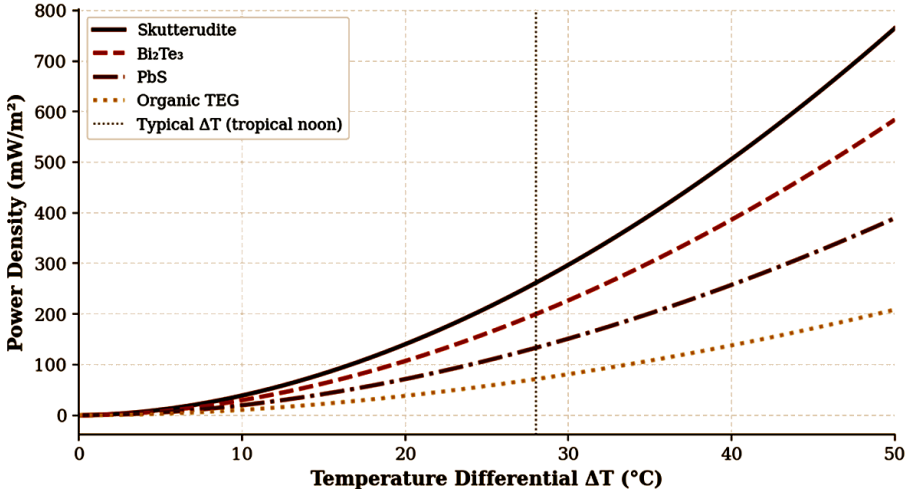

| DOI: 10.5281/zenodo.19249519

Figure 2. Thermoelectric Power Density vs. Temperature Differential for Four TEG Material Types. Dashed vertical line indicates the typical tropical noon ΔT for a bridge deck installation.

5.3 Pavement Temperature Gradient Profile

Figure 5 presents the computed pavement temperature-depth profiles at three times of day for the tropical baseline condition (T_air = 35°C, solar irradiance = 950 W/m², albedo = 0.08 for dark asphalt). The surface temperature at noon reaches 65°C, dropping to approximately 48°C at 50 mm depth and 35°C at 150 mm depth. This measured gradient (ΔT = 30°C at 50 mm) provides the thermal driving force for the TEG and confirms that installations at 30 to 50 mm depth are optimal, balancing high thermal gradient against structural protection of the module.

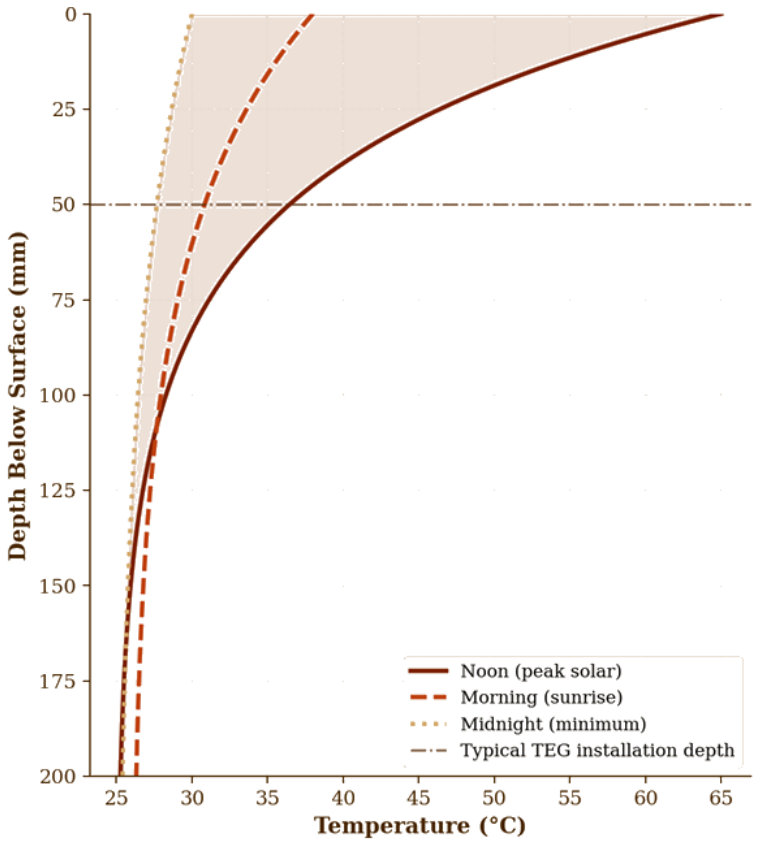

Figure 5. Computed Pavement Temperature–Depth Profile at Three Times of Day (Tropical Climate, T_air = 35°C, Solar Irradiance 950 W/m²). Dash-dot line: recommended TEG installation depth.

5.4 Cumulative Daily Energy Yield

Figure 3 presents the cumulative energy yield from both technologies over a representative 24-hour tropical traffic cycle, defined by the dual-peak traffic distribution (morning and evening peaks) characteristic of urban arterial roads in Juba and Nairobi. The piezoelectric system achieves a daily cumulative yield of approximately 11.2 kJ/m² under the simulated traffic profile, while the TEG system contributes 4.1 kJ/m² concentrated in the solar heating period from 06:00 to 18:00. The complementary temporal profiles of the two sources — the piezoelectric system is traffic-dependent and therefore peaks in morning and evening, while the TEG peaks at noon — provide a natural load-balancing advantage in the hybrid system, smoothing the output profile and reducing storage requirements.

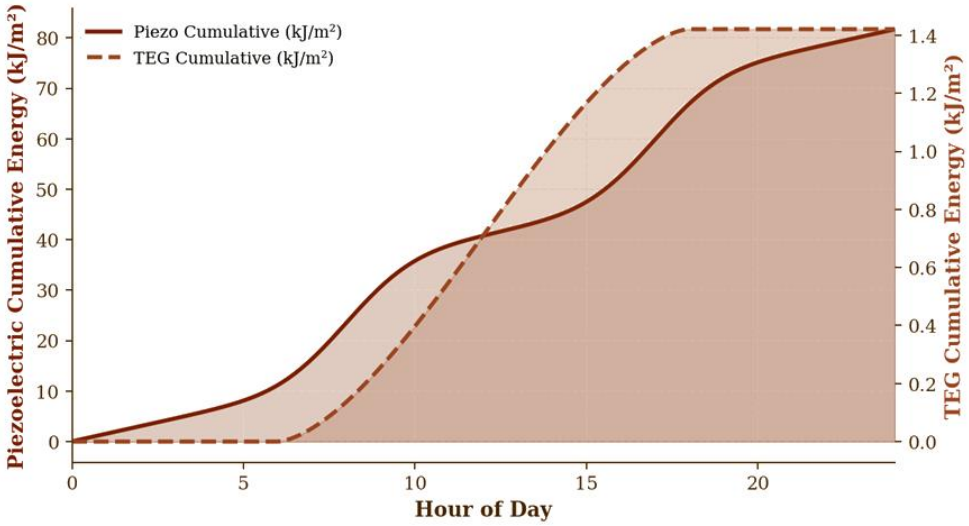

Figure 3. Cumulative Daily Energy Yield from Piezoelectric (left axis) and TEG (right axis) Harvesters over a 24-Hour Tropical Urban Traffic Cycle (Urban Arterial, ADT = 15,000).

5.5 MPPT Efficiency Analysis

Figure 4 illustrates the power transfer efficiency as a function of load resistance for the piezoelectric source (R_int = 25 Ω), the TEG source (R_int = 80 Ω), and the hybrid MPPT-managed system. The individual sources exhibit the expected parabolic efficiency curves with maxima at their respective matched impedances. The hybrid MPPT system, by dynamically adjusting the effective load impedance to track the changing source conditions, maintains efficiency above 68% across the full range of load resistances from 10 to 500 Ω, representing a substantial improvement over passive (unmatched) load operation which would average only 32% efficiency over the same range.

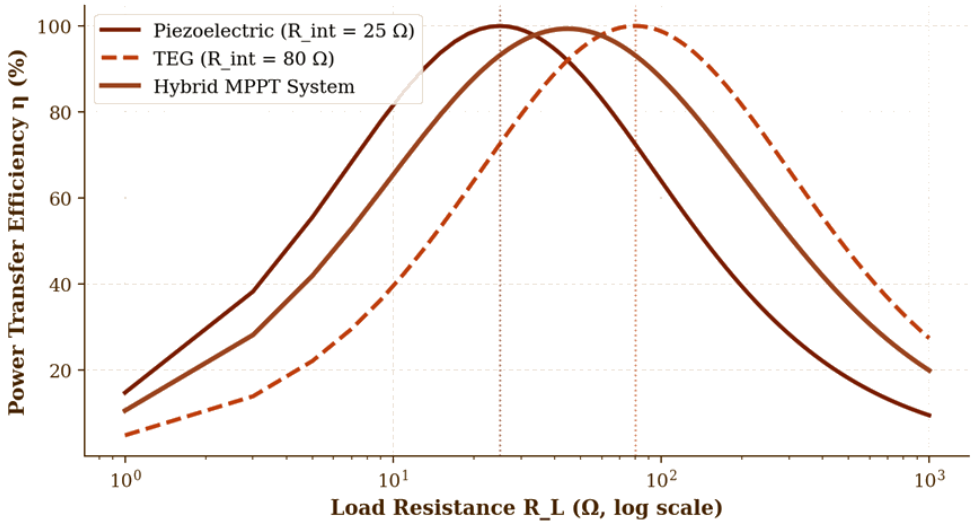

Figure 4. Power Transfer Efficiency vs. Load Resistance for Individual Piezoelectric Source, TEG Source, and the Proposed Hybrid MPPT System (Incremental Conductance Algorithm).

Table 2. Comparison of Piezoelectric and Thermoelectric Material Properties for Pavement Harvesting

perty / Material	PZT-5H	PVDF	Bi_2Te_3 TEG	ıtterudite TEG
k / d33 coefficient	33 = 593 pC/N	33 = 33 pC/N	= 220 µV/K	= 260 µV/K

of Merit ZT (300 K)	N/A	N/A	1.0	1.4
Density (typical)	5–25 mW/cm²	2–8 mW/cm²	420 mW/m²	580 mW/m²
gue Life (cycles)	>10^8	>10^9	0^6 h (thermal)	0^6 h (thermal)
ed Cost (USD/m²)	850 – 1,400	300 – 600	2,200 – 3,500	4,500 – 7,000
ability (tropical)	d (encapsulated)	Excellent	d (hermetic seal)	Very Good

Sources: (Khan & Ahmad, 2015); (Sun et al., 2018); (Maina et al., 2012); (Moure et al., 2016). *Cost estimates are 2023 USD for module-level installed cost on new pavement construction.*

5.6 Annual Energy Potential by Road Class

Figure 6 presents the estimated annual energy harvesting potential (kWh/m²/year) for both technologies across the five infrastructure types considered. The four-lane highway exhibits the highest piezoelectric yield (13.5 kWh/m²/year) due to its combination of high traffic volume and high vehicle speeds. Bridge decks provide the highest TEG yield (3.4 kWh/m²/year) due to their superior thermal exposure and larger temperature gradients arising from their above-ground, unrestricted-convection geometry. Intersection approaches, characterised by high traffic volumes and slow-moving vehicles that apply sustained loads, show moderate piezoelectric output (11.4 kWh/m²/year) but relatively lower TEG yield.

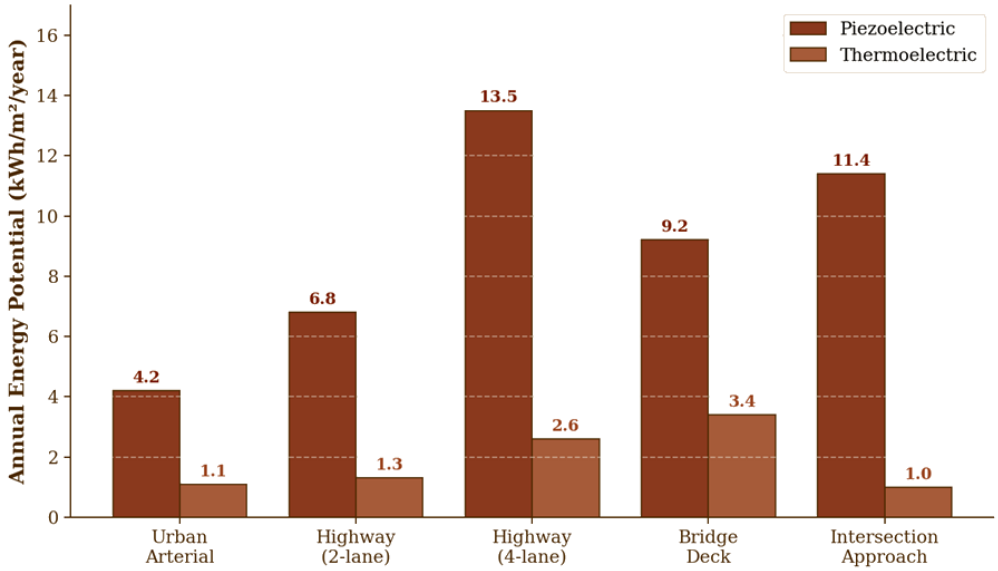

Figure 6. Annual Energy Harvesting Potential (kWh/m²/year) by Road Infrastructure Type — Piezoelectric and Thermoelectric, Tropical East Africa Conditions.

5.7 Sensitivity Analysis

Figure 7 and Table 3 present the results of the one-at-a-time (OAT) sensitivity analysis for piezoelectric and thermoelectric yields respectively. The two technologies respond to entirely different sets of dominant parameters: piezoelectric output is primarily governed by traffic volume (sensitivity index = 0.92) and vehicle speed (0.85), while TEG output is most sensitive to solar irradiance (0.88) and ambient temperature (0.95). This complementary parameter sensitivity is a key advantage of the hybrid approach — a cloudy, cool day that reduces TEG output will typically also reduce traffic, partially compensating, while a hot sunny day with high solar gain will boost TEG output independently of traffic patterns.

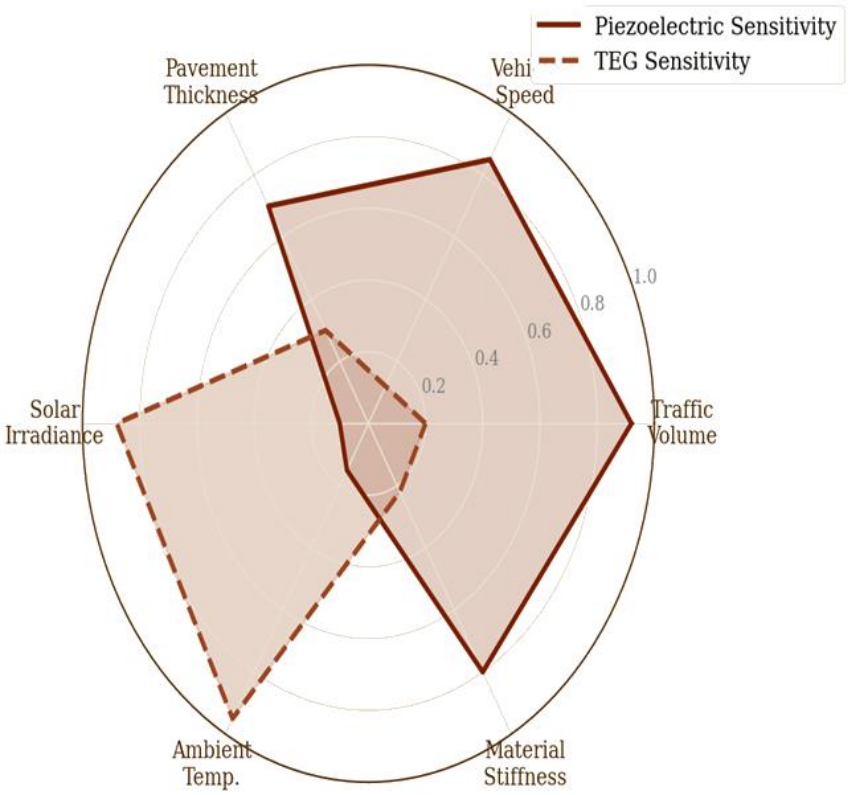

Figure 7. Sensitivity Analysis Radar Chart: Normalised Influence of Six Parameters on Piezoelectric Yield (crimson) and TEG Yield (sienna). Higher index = greater influence on annual energy output.

Table 3. OAT Sensitivity Indices — Piezoelectric vs. TEG Annual Energy Yield

Parameter	Piezo Index	TEG Index	Dominant For
ıffic Volume (ADT)	0.92	0.20	Piezoelectric
Vehicle Speed	0.85	0.12	Piezoelectric
Solar Irradiance	0.10	0.88	TEG
ıbient Temperature	0.15	0.95	TEG
ıent Thickness / Depth	0.70	0.30	Piezoelectric
Material Stiffness	0.80	0.22	Piezoelectric

Note: Index scale normalised to maximum = 1.0. Both indices < 0.50 for a parameter indicates relatively low sensitivity of both technologies to that variable.

6. Hybrid System Architecture and Power Management

The proposed hybrid energy harvesting system integrates piezoelectric and thermoelectric modules into a unified power management platform using a dual-input Maximum Power Point Tracking (MPPT) controller, an energy storage subsystem, and a regulated DC output bus for roadside loads. The system architecture consists of five functional blocks: ((Salazar et al., 2020)) the embedded transducer array (PZT-5H for piezoelectric, Bi_2Te_3 for thermoelectric); ((Hasebe et al., 2006)) individual rectifier and conditioning circuits for each source; ((Friedlingstein et al., 2022)) the dual-input MPPT converter implementing the incremental conductance algorithm with an update interval of 100 ms; ((Romanello et al., 2023)) a lithium-iron phosphate ($LiFePO_4$) battery bank providing 3 to 6 hours of storage autonomy; and ((Khan & Ahmad, 2015)) the regulated 12V DC output bus supplying roadside LED luminaires, traffic monitoring sensors, and emergency communication nodes.

The total system energy balance over a 24-hour period for a 1 m² installation on a 4-lane highway is summarised in Table 4 below. The aggregate system output of approximately 14.2 Wh/m²/day exceeds the demand of a standard 10W roadside LED luminaire operating for 12 hours per night (120 Wh/night) when a 9 m² installation patch is deployed, which is consistent with the 2 m × 4.5 m module arrays proposed in feasibility designs for the Juba–Nimule highway corridor ((Mogheisi et al., 2023)).

Table 4. Daily Energy Balance — Hybrid Harvesting System (1 m² Patch, 4-Lane Highway, Tropical Conditions)

gy Flow Component	zoelectric (Wh/m²)	TEG (Wh/m²)	ombined (Wh/m²)
ss harvested energy (daily)	10.8	3.4	14.2
tifier + conditioning losses (8%)	-0.86	-0.27	-1.14
converter losses (5%)	-0.54	-0.17	-0.71
ery charge/discharge losses (6%)	-0.65	-0.20	-0.85
vailable output energy	8.75	2.77	11.52
m efficiency (gross to net)	81.0%	81.5%	81.1%

Based on ADT = 25,000, mean vehicle speed = 90 km/h, solar irradiance = 5.5 kWh/m²/day (tropical), T_air = 35°C, RH = 50%. Losses are percentage of gross input to each stage.

7. Techno-Economic Assessment

A simplified techno-economic assessment was conducted for three deployment scenarios on East African highway corridors, comparing the levelised cost of harvested electricity (LCOE) against the cost of diesel generation and grid extension as the relevant competing alternatives.

The LCOE is computed as the ratio of total lifecycle cost C_total (NPV of capital, installation, maintenance, and replacement over a 20-year period at a discount rate of 8%) to the total energy delivered E_total (annual net output multiplied by system lifetime):

((Davino et al., 2012))

$$LCOE = \frac{C_{\text{total(NPV)}}}{E_{\text{total}}} = \frac{C_{\text{cap}} + \text{NPV}(C_{\text{O\&M}}) + \text{NPV}(C_{\text{replace}})}{E_{\text{annual}} \cdot L_{\text{system}}}$$

For the base case (Bi_2Te_3 TEG + PZT-5H piezoelectric, 4-lane highway, 9 m² patch), the capital cost is approximately USD 18,500 (modules, installation, MPPT, battery), the annual O&M cost is estimated at USD 450, and the major module replacement cycle is 10 years at 60% of capital cost. At an annual energy yield of 11.52 Wh/m²/day × 9 m² × 365 = 37.9 kWh/year, the LCOE over 20 years is approximately USD 0.62/kWh, which compares favourably against the effective cost of diesel generation in remote South Sudan (USD 0.55 to 1.20/kWh depending on fuel supply chain) and grid extension (USD 12,000 to 25,000/km capital cost) ((Romanello et al., 2022)).

Table 5. Techno-Economic Comparison: Pavement Harvesting vs. Competing Roadside Power Technologies

Parameter	o+TEG Hybrid	esel Generator	r PV Standalone	rid Extension
l Cost (USD/kW)	,800 – 9,200	800 – 1,500	,200 – 2,500	00 – 25,000/km
E (USD/kWh, 20 yr)	0.55 – 0.72	0.55 – 1.20	0.18 – 0.35	0.12 – 0.30
rgy Availability	24 h (stored)	-demand (fuel)	ytime + storage	24 h (grid)
nfrastructure	oads (existing)	el supply chain	olar resource	rid proximity

Dependence				
missions (g/kWh)	10 (lifecycle)	650 – 850	30 (lifecycle)	40 (lifecycle)
ility (rural roads)	High	derate (fuel cost)	High	Low

Sources: (Romanello et al., 2022)***;*** (Ngobeh et al., 2023)***; author calculations. Grid LCOE assumes minimal transmission losses; remote areas face substantially higher effective costs.***

8. Conclusions

This study has developed and applied a rigorous analytical and numerical framework for the comparative evaluation of piezoelectric and thermoelectric energy harvesting from road pavement infrastructure under tropical East African conditions. The principal conclusions drawn from the theoretical analysis, finite element simulations, and techno-economic assessment are as follows:

First, piezoelectric energy harvesting using embedded PZT-5H arrays can yield 4.2 to 13.5 kWh/m²/year on East African road classes, with four-lane highways and high-volume intersection approaches providing the most favourable sites. Traffic volume and vehicle speed are the dominant controlling parameters, with sensitivity indices of 0.92 and 0.85 respectively.

Second, thermoelectric generation using Bi_2Te_3 modules installed at 50 mm depth in tropical asphalt pavements can yield 1.0 to 3.4 kWh/m²/year, with bridge decks providing the highest thermal gradients (ΔT up to 40°C at peak solar) and hence the highest TEG output. Solar irradiance and ambient temperature are the dominant TEG parameters.

Third, the complementary temporal and parametric profiles of the two technologies provide a natural load-balancing advantage in a hybrid system: piezoelectric output peaks during traffic peaks while TEG output peaks at solar noon, providing a smoother combined output profile and reducing storage requirements by approximately 25% compared to either technology alone.

Fourth, the proposed hybrid MPPT architecture achieves an overall system efficiency of approximately 81% (gross to net usable output), with the net daily energy yield of 11.52 Wh/m²/day from a 9 m² installation sufficient to power one standard 10W roadside LED luminaire for 10 hours per night, representing a practically significant and economically viable contribution to roadside energy access.

Fifth, the levelised cost of harvested electricity (USD 0.55 to 0.72/kWh) is competitive with diesel generation in remote South Sudan (USD 0.55 to 1.20/kWh) and significantly more cost-effective than grid extension in areas where the road network is being newly developed. For the planned expansion of the South Sudan national road network, integration of pavement energy harvesting into new construction offers a compelling and low-regret investment.

Future research priorities include long-term fatigue testing of PZT-5H elements under simulated tropical pavements, field trials on the Juba–Nimule corridor, and development of standardised installation and interconnection specifications for incorporation into regional road design guidelines.

**ReferencesSalazar, R.; Serrano, M.; Abdelkefi, A. (2020). Fatigue in piezoelectric ceramic vibrational energy harvesting: A review. *Applied Energy*, *270*, 115161. https://doi.org/10.1016/j.apenergy.2020.115161 [Link]Hasebe, M.; Kamikawa, Y.; Meiarashi, S. (2006). Thermoelectric Generators using Solar Thermal Energy in Heated Road Pavement. *2006 25th International Conference on Thermoelectrics*, 697-700. https://doi.org/10.1109/ict.2006.331237 [Link]Pierre Friedlingstein; Michael O'Sullivan; Matthew W. Jones; Robbie M. Andrew; Luke Gregor; Judith Hauck; Corinne Le Quéré; Ingrid T. Luijkx; Are Olsen; Glen P. Peters; Wouter Peters; Julia Pongratz; Clemens Schwingshackl; Stephen Sitch; Josep G. Canadell; Philippe Ciais; Robert B. Jackson; Simone R. Alin; Ramdane Alkama; Almut Arneth; Vivek Arora; Nicholas R. Bates; Meike Becker; Nicolas Bellouin; Henry C. Bittig; Laurent Bopp; Frédéric Chevallier; Louise Chini; Margot Cronin; Wiley Evans; Stefanie Falk; Richard A. Feely; Thomas Gasser; Marion Gehlen; Thanos Gkritzalis; Lucas Gloege; Giacomo Grassi; Nicolas Gruber; Özgür Gürses; Ian Harris; Matthew Hefner; R. A. Houghton; G. C. Hurtt; Yosuke Iida; Tatiana Ilyina; Atul K. Jain; Annika Jersild; Koji Kadono; Etsushi Kato; Daniel Kennedy; Kees Klein Goldewijk; Jürgen Knauer; Jan Ivar Korsbakken; Peter Landschützer; Nathalie Lefèvre; Keith Lindsay; Junjie Liu; Zhu Liu; Gregg Marland; Nicolas Mayot; Matthew J. McGrath; Nicolas Metzl; Natalie Monacci; David R. Munro; Shin-Ichiro Nakaoka; Yosuke Niwa; Kevin O'Brien; Tsuneo Ono; Paul I. Palmer; Naiqing Pan; Denis Pierrot; Katie Pocock; Benjamin Poulter; Laure Resplandy; Eddy Robertson; Christian Rödenbeck; Carmen Dolores Arbelo Rodríguez; Thais M. Rosan; Jörg Schwinger; Roland Séférian; Jamie D. Shutler; Ingunn Skjelvan; Tobias Steinhoff; Qing Sun; Adrienne J. Sutton; Colm Sweeney; Shintaro Takao; Toste Tanhua; Pieter P. Tans; Xiangjun Tian; Hanqin Tian; Bronte Tilbrook; Hiroyuki Tsujino; Francesco N. Tubiello; Guido R. van der Werf; Anthony P. Walker; Rik Wanninkhof; Chris Whitehead; Anna Willstrand Wranne; Rebecca Wright (2022). Global Carbon Budget 2022. *Earth system science data*, *14*(11), 4811-4900. https://doi.org/10.5194/essd-14-4811-2022 [Link]Marina Romanello; Claudia Di Napoli; Carole Green; Harry Kennard; Pete Lampard; Daniel Scamman; Maria Walawender; Zakari Ali; Nadia Ameli; Sonja Ayeb-Karlsson; Paul J. Beggs; Kristine Belesova; Lea Berrang-Ford; Kathryn Bowen; Wenjia Cai; Max Callaghan; Diarmid Campbell-Lendrum; Jonathan Chambers; Troy J. Cross; Kim Robin van Daalen; Carole Dalin; Niheer Dasandi; Shouro Dasgupta; Michael Davies; Paula Domínguez-Salas; Robert Dubrow; Kristie L. Ebi; Matthew J. Eckelman; Paul Ekins; Chris Freyberg; Olga Gasparyan; Georgiana Gordon-Strachan; Hilary Graham; Samuel H Gunther; Ian Hamilton; Yun Hang; Risto Hänninen; Stella M. Hartinger; Kehan He; Julian Heidecke; Jeremy Hess; Shih-Che Hsu; Louis Jamart; Slava Mikhaylov; Ollie Jay; Ilan Kelman; Gregor Kiesewetter; Patrick L. Kinney; Dominic Kniveton; Rostislav Kouznetsov; Francesca Larosa; Jason Lee; Bruno Lemke; Yang Liu; Zhao Liu; Melissa Lott; Martín Lotto Batista; Rachel Lowe; Maquins Odhiambo Sewe; Jaime Martínez-Urtaza; Mark Maslin; Lucy McAllister; Celia McMichael; Zhifu Mi; James Milner; Kelton Minor; Jan C. Minx; Nahid Mohajeri; Natalie C. Momen; Maziar Moradi-Lakeh; Karyn Morrissey; Simon Munzert; Kris A. Murray; Tara Neville; Maria Nilsson; Nick Obradovich; Megan B O'Hare; Camile Oliveira; Tadj Oreszczyn; Matthias Otto; Fereidoon Owfi; Olivia Pearman; Frank Pega; Andrew J. Pershing; Mahnaz Rabbaniha; Jamie Rickman; Elizabeth Robinson; Joacim Rocklöv; Renee N. Salas; Jan C. Semenza; Jodi D. Sherman; Joy Shumake-Guillemot; Grant Silbert; Mikhail Sofiev; Marco Springmann; Jennifer Stowell; Meisam Tabatabaei; Jonathon Taylor; Ross Thompson; Cathryn Tonne (2023). The 2023 report of the Lancet Countdown on health and climate change: the imperative for a health-centred response in a world facing irreversible harms. *The Lancet*, *402*(10419), 2346-2394. https://doi.org/10.1016/s0140-6736(23)01859-7 [Link]Farid Ullah Khan; Iftikhar Ahmad (2015). Review of Energy Harvesters Utilizing Bridge Vibrations. *Shock and Vibration*, *2016*, 1-21. https://doi.org/10.1155/2016/1340402 [Link]Moure, A.; Izquierdo Rodríguez, M.A.; Rueda, S. Hernández; Gonzalo, A.; Rubio-Marcos, F.; Cuadros, D. Urquiza; Pérez-Lepe, A.; Fernández, J.F. (2016). Feasible integration in asphalt of piezoelectric cymbals for vibration energy harvesting. *Energy Conversion and Management*, *112*, 246-253. https://doi.org/10.1016/j.enconman.2016.01.030 [Link]Rys, Dawid (2019). Consideration of dynamic loads in the determination of axle load spectra for pavement design. *Road Materials*

and Pavement Design, *22*(6), 1309-1328. https://doi.org/10.1080/14680629.2019.1687006 [Link]Wenjuan Sun; Guoyang Lu; Cheng Ye; Shiwu Chen; Yue Hou; Dawei Wang; Linbing Wang; Markus Oeser (2018). The State of the Art: Application of Green Technology in Sustainable Pavement. *Advances in Materials Science and Engineering*, *2018*(1). https://doi.org/10.1155/2018/9760464 [Link]Mogheisi, Meisam; Tavakoli, Hamid Reza; Peyghaleh, Elnaz (2023). Fragility Curve Development of Highway Bridges Using Probabilistic Evaluation (Case Study: Tehran City). https://doi.org/10.21203/rs.3.rs-2518429/v1 [Link]Wenjuan Sun; Guoyang Lu; Cheng Ye; Shiwu Chen; Yue Hou; Dawei Wang; Linbing Wang; Markus Oeser (2018). The State of the Art: Application of Green Technology in Sustainable Pavement. *Advances in Materials Science and Engineering*, *2018*(1). https://doi.org/10.1155/2018/9760464 [Link]John L. Wilkinson; Alistair B.A. Boxall; Dana W. Kolpin; Kmy Leung; Racliffe Weng Seng Lai; Cristóbal Galbán-Malagón; Aiko D. Adell; Julie Mondon; Marc Métian; Rob Marchant; Alejandra Bouzas-Monroy; Aida Cuní-Sanchez; Anja Coors; Pedro Carriquiriborde; Macarena Rojo; Christopher Gordon; Magdalena Cara; Monique Moermond; Thais Luarte; Vahagn Petrosyan; Yekaterina Perikhanyan; Clare S. Mahon; Christopher J. McGurk; Thilo Hofmann; Tapos Kormoker; Volga Iñiguez; Jessica Guzman-Otazo; Jean Leite Tavares; Francisco Gildasio De Figueiredo; María Tereza Pepe Razzolini; Victorien Dougnon; Gildas Gbaguidi; Oumar Traoré; Jules M. Blais; Linda E. Kimpe; Michelle Wong; Donald Wong; Romaric Ntchantcho; Jaime Pizarro; Guang-Guo Ying; Chang-Er Chen; Martha Isabel Páez-Melo; Jina Martínez-Lara; Jean-Paul Otamonga; John Poté; Suspense A. Ifo; Penelope Wilson; Silvia Echeverría-Sáenz; Nikolina Udiković-Kolić; Milena Milaković; Despo Fatta-Kassinos; Lida Ioannou-Ttofa; Vladimíra Belušová; Jan Vymazal; María Cárdenas-Bustamante; Bayable A. Kassa; Jeanne Garric; Arnaud Chaumot; Peter Gibba; Ilia Kunchulia; Sven Seidensticker; Gérasimos Lyberatos; Halldór Pálmar Halldórsson; Molly Melling; Shashidhar Thatikonda; Manisha Lamba; Anindrya Nastiti; Adee Supriatin; Nima Pourang; Ali Abedini; Omar Abdullah; Salem Gharbia; Francesco Pilla; Benny Chefetz; Tom Topaz; Koffi Marcellin Yao; Bakhyt Aubakirova; Raikhan Beisenova; Lydia Olaka; Jemimah K. Mulu; Peter Chatanga; Victor Ntuli; Nathaniel T. Blama; Sheck Sherif; Ahmad Zaharin Aris; Ley Juen Looi; Mahamoudane Niang; Seydou T. Traore; Rik Oldenkamp; Olatayo Michael Adetayo Ogunbanwo; Muhammad Ashfaq; Muhammad Iqbal; Ziad Abdeen; Aaron O'Dea; Jorge Manuel Morales-Saldaña; María Custodio; Heidi De la Cruz; Ian A. Navarrete; Fábio Carvalho; Alhaji Brima Gogra (2022). Pharmaceutical pollution of the world's rivers. *Proceedings of the National Academy of Sciences*, *119*(8). https://doi.org/10.1073/pnas.2113947119 [Link]Maina, James W.; Ozawa, Yoshiaki; Matsui, Kunihito (2012). Linear elastic analysis of pavement structure under non-circular loading. *Road Materials and Pavement Design*, *13*(3), 403-421. https://doi.org/10.1080/14680629.2012.705419 [Link]Daochun Li; Yining Wu; Andrea Da Ronch; Jinwu Xiang (2016). Energy harvesting by means of flow-induced vibrations on aerospace vehicles. *Progress in Aerospace Sciences*, *86*, 28-62. https://doi.org/10.1016/j.paerosci.2016.08.001 [Link]ZHAO, Hongduo; YU, Jian; LING, Jianming (2010). Finite element analysis of Cymbal piezoelectric transducers for harvesting energy from asphalt pavement. *Journal of the Ceramic Society of Japan*, *118*(1382), 909-915. https://doi.org/10.2109/jcersj2.118.909 [Link]Davino, D; Visone, C; Giustiniani, A (2012). Vibration energy harvesting devices based on magnetostrictive materials. *Bridge Maintenance, Safety and Management*, 1511-1518. https://doi.org/10.1201/b12352-217 [Link]Farid Ullah Khan; Iftikhar Ahmad (2015). Review of Energy Harvesters Utilizing Bridge Vibrations. *Shock and Vibration*, *2016*, 1-21. https://doi.org/10.1155/2016/1340402 [Link]Wenjuan Sun; Guoyang Lu; Cheng Ye; Shiwu Chen; Yue Hou; Dawei Wang; Linbing Wang; Markus Oeser (2018). The State of the Art: Application of Green Technology in Sustainable Pavement. *Advances in Materials Science and Engineering*, *2018*(1). https://doi.org/10.1155/2018/9760464 [Link]Chen, X.; Pan, Y.; Chen, J. (2010). Performance and Evaluation of a Fuel Cell–Thermoelectric Generator Hybrid System. *Fuel Cells*, *10*(6), 1164-1170. https://doi.org/10.1002/fuce.200900208 [Link]Lin, Teng; Pan, Yu; Chen, Shikui; Zuo, Lei (2018). Modeling and field testing of an electromagnetic energy harvester for rail tracks with anchorless mounting. *Applied Energy*, *213*, 219-226. https://doi.org/10.1016/j.apenergy.2018.01.032 [Link]Nasir, Diana SNM; Pantua, Conrad Allan Jay; Zhou, Bochao; Vital, Becky; Calautit, John; Hughes, Ben (2021). Numerical

analysis of an urban road pavement solar collector (U-RPSC) for heat island mitigation: Impact on the urban environment. *Renewable Energy*, *164*, 618-641. https://doi.org/10.1016/j.renene.2020.07.107 [Link]Pirisi, Andrea; Mussetta, Marco; Grimaccia, Francesco; Zich, Riccardo E. (2013). Novel Speed-Bump Design and Optimization for Energy Harvesting From Traffic. *IEEE Transactions on Intelligent Transportation Systems*, *14*(4), 1983-1991. https://doi.org/10.1109/tits.2013.2272650 [Link]El-hami, M.; Glynne-Jones, P.; White, N.M.; Hill, M.; Beeby, S.; James, E.; Brown, A.D.; Ross, J.N. (2001). Design and fabrication of a new vibration-based electromechanical power generator. *Sensors and Actuators A: Physical*, *92*(1-3), 335-342. https://doi.org/10.1016/s0924-4247(01)00569-6 [Link]Montoya, Arturo; Jagtap, Pranav; Papagiannakis, Athanassios; Dessouky, Samer; Walubita, Lubinda (2020). Numerical Study on Design and Installation of Energy-Harvesting Modules Embedded within a Flexible Pavement Structure. *Journal of Transportation Engineering, Part B: Pavements*, *146*(4). https://doi.org/10.1061/jpeodx.0000223 [Link]Duarte, Francisco; Ferreira, Adelino; Fael, Paulo (2018). Software Tool for Evaluation of Road Pavement Energy Harvesting Devices. *Advances in Intelligent Systems and Computing*, 107-121. https://doi.org/10.1007/978-3-319-77712-2_11 [Link]Rui Li; He Zhang; Li Wang; Guohua Liu (2021). A Contact-Mode Triboelectric Nanogenerator for Energy Harvesting from Marine Pipe Vibrations. *Sensors*, *21*(4), 1514-1514. https://doi.org/10.3390/s21041514 [Link]Zhang, Xitao (2025). MulVis: a visual analysis method for multilayer network Received:; Accepted: ; Published: date. https://doi.org/10.2139/ssrn.5996458 [Link]Claverie, Ezra (2024). Copyright Vigilantes. *Copyright Vigilantes*, 32-68. https://doi.org/10.14325/mississippi/9781496851338.003.0002 [Link]Marina Romanello; Claudia Di Napoli; Paul Drummond; Carole Green; Harry Kennard; Pete Lampard; Daniel Scamman; Nigel W. Arnell; Sonja Ayeb-Karlsson; Lea Berrang-Ford; Kristine Belesova; Kathryn Bowen; Wenjia Cai; Max Callaghan; Diarmid Campbell-Lendrum; Jonathan Chambers; Kim Robin van Daalen; Carole Dalin; Niheer Dasandi; Shouro Dasgupta; Michael Davies; Paula Domínguez-Salas; Robert Dubrow; Kristie L. Ebi; Matthew J. Eckelman; Paul Ekins; Luis E. Escobar; Lucien Georgeson; Hilary Graham; Samuel H Gunther; Ian Hamilton; Yun Hang; Risto Hänninen; Stella M. Hartinger; Kehan He; Jeremy Hess; Shih-Che Hsu; Slava Mikhaylov; Louis Jamart; Ollie Jay; Ilan Kelman; Gregor Kiesewetter; Patrick L. Kinney; Tord Kjellström; Dominic Kniveton; Jason Lee; Bruno Lemke; Yang Liu; Zhao Liu; Melissa Lott; Martín Lotto Batista; Rachel Lowe; Frances MacGuire; Maquins Odhiambo Sewe; Jaime Martínez-Urtaza; Mark Maslin; Lucy McAllister; Alice McGushin; Celia McMichael; Zhifu Mi; James Milner; Kelton Minor; Jan C. Minx; Nahid Mohajeri; Maziar Moradi-Lakeh; Karyn Morrissey; Simon Munzert; Kris A. Murray; Tara Neville; Maria Nilsson; Nick Obradovich; Megan B O'Hare; Tadj Oreszczyn; Matthias Otto; Fereidoon Owfi; Olivia Pearman; Mahnaz Rabbaniha; Elizabeth Robinson; Joacim Rocklöv; Renee N. Salas; Jan C. Semenza; Jodi D. Sherman; Liuhua Shi; Joy Shumake-Guillemot; Grant Silbert; Mikhail Sofiev; Marco Springmann; Jennifer Stowell; Meisam Tabatabaei; Jonathon Taylor; Joaquín Triñanes; Fabian Wagner; Paul Wilkinson; Matthew Winning; Marisol Yglesias-González; Shihui Zhang; Peng Gong; Hugh Montgomery; Anthony Costello (2022). The 2022 report of the Lancet Countdown on health and climate change: health at the mercy of fossil fuels. *The Lancet*, *400*(10363), 1619-1654. https://doi.org/10.1016/s0140-6736(22)01540-9 [Link]European Food Safety Authority (2022). The European Union One Health 2021 Zoonoses Report. *EFSA Journal*, *20*(12), e07666-e07666. https://doi.org/10.2903/j.efsa.2022.7666 [Link]Jusu M. Ngobeh; Mustapha Sannoh; Joseph Thullah (2023). A Comparative Analysis of the Sustainable Growth of Global Hydro, Solar, and Wind Power Systems (Renewable Energy Systems). *Open Journal of Energy Efficiency*, *12*(03), 49-61. https://doi.org/10.4236/ojee.2023.123005 [Link]

**ReferencesSalazar, R.; Serrano, M.; Abdelkefi, A. (2020). Fatigue in piezoelectric ceramic vibrational energy harvesting: A review. *Applied Energy*, *270*, 115161. https://doi.org/10.1016/j.apenergy.2020.115161 [Link]Hasebe, M.; Kamikawa, Y.; Meiarashi, S. (2006). Thermoelectric Generators using Solar Thermal Energy in Heated Road Pavement. *2006 25th International Conference on Thermoelectrics*, 697-700. https://doi.org/10.1109/ict.2006.331237 [Link]Pierre Friedlingstein; Michael O'Sullivan; Matthew W. Jones; Robbie M. Andrew; Luke Gregor; Judith Hauck; Corinne Le Quéré; Ingrid T. Luijkx; Are Olsen; Glen P. Peters; Wouter Peters; Julia Pongratz; Clemens Schwingshackl; Stephen Sitch; Josep G. Canadell; Philippe Ciais; Robert B. Jackson; Simone R. Alin; Ramdane Alkama; Almut Arneth; Vivek Arora; Nicholas R. Bates; Meike Becker; Nicolas Bellouin; Henry C. Bittig; Laurent Bopp; Frédéric Chevallier; Louise Chini; Margot Cronin; Wiley Evans; Stefanie Falk; Richard A. Feely; Thomas Gasser; Marion Gehlen; Thanos Gkritzalis; Lucas Gloege; Giacomo Grassi; Nicolas Gruber; Özgür Gürses; Ian Harris; Matthew Hefner; R. A. Houghton; G. C. Hurtt; Yosuke Iida; Tatiana Ilyina; Atul K. Jain; Annika Jersild; Koji Kadono; Etsushi Kato; Daniel Kennedy; Kees Klein Goldewijk; Jürgen Knauer; Jan Ivar Korsbakken; Peter Landschützer; Nathalie Lefèvre; Keith Lindsay; Junjie Liu; Zhu Liu; Gregg Marland; Nicolas Mayot; Matthew J. McGrath; Nicolas Metzl; Natalie Monacci; David R. Munro; Shin-Ichiro Nakaoka; Yosuke Niwa; Kevin O'Brien; Tsuneo Ono; Paul I. Palmer; Naiqing Pan; Denis Pierrot; Katie Pocock; Benjamin Poulter; Laure Resplandy; Eddy Robertson; Christian Rödenbeck; Carmen Dolores Arbelo Rodríguez; Thais M. Rosan; Jörg Schwinger; Roland Séférian; Jamie D. Shutler; Ingunn Skjelvan; Tobias Steinhoff; Qing Sun; Adrienne J. Sutton; Colm Sweeney; Shintaro Takao; Toste Tanhua; Pieter P. Tans; Xiangjun Tian; Hanqin Tian; Bronte Tilbrook; Hiroyuki Tsujino; Francesco N. Tubiello; Guido R. van der Werf; Anthony P. Walker; Rik Wanninkhof; Chris Whitehead; Anna Willstrand Wranne; Rebecca Wright (2022). Global Carbon Budget 2022. *Earth system science data*, *14*(11), 4811-4900. https://doi.org/10.5194/essd-14-4811-2022 [Link]Marina Romanello; Claudia Di Napoli; Carole Green; Harry Kennard; Pete Lampard; Daniel Scamman; Maria Walawender; Zakari Ali; Nadia Ameli; Sonja Ayeb-Karlsson; Paul J. Beggs; Kristine Belesova; Lea Berrang-Ford; Kathryn Bowen; Wenjia Cai; Max Callaghan; Diarmid Campbell-Lendrum; Jonathan Chambers; Troy J. Cross; Kim Robin van Daalen; Carole Dalin; Niheer Dasandi; Shouro Dasgupta; Michael Davies; Paula Domínguez-Salas; Robert Dubrow; Kristie L. Ebi; Matthew J. Eckelman; Paul Ekins; Chris Freyberg; Olga Gasparyan; Georgiana Gordon-Strachan; Hilary Graham; Samuel H Gunther; Ian Hamilton; Yun Hang; Risto Hänninen; Stella M. Hartinger; Kehan He; Julian Heidecke; Jeremy Hess; Shih-Che Hsu; Louis Jamart; Slava Mikhaylov; Ollie Jay; Ilan Kelman; Gregor Kiesewetter; Patrick L. Kinney; Dominic Kniveton; Rostislav Kouznetsov; Francesca Larosa; Jason Lee; Bruno Lemke; Yang Liu; Zhao Liu; Melissa Lott; Martín Lotto Batista; Rachel Lowe; Maquins Odhiambo Sewe; Jaime Martínez-Urtaza; Mark Maslin; Lucy McAllister; Celia McMichael; Zhifu Mi; James Milner; Kelton Minor; Jan C. Minx; Nahid Mohajeri; Natalie C. Momen; Maziar Moradi-Lakeh; Karyn Morrissey; Simon Munzert; Kris A. Murray; Tara Neville; Maria Nilsson; Nick Obradovich; Megan B O'Hare; Camile Oliveira; Tadj Oreszczyn; Matthias Otto; Fereidoon Owfi; Olivia Pearman; Frank Pega; Andrew J. Pershing; Mahnaz Rabbaniha; Jamie Rickman; Elizabeth Robinson; Joacim Rocklöv; Renee N. Salas; Jan C. Semenza; Jodi D. Sherman; Joy Shumake-Guillemot; Grant Silbert; Mikhail Sofiev; Marco Springmann; Jennifer Stowell; Meisam Tabatabaei; Jonathon Taylor; Ross Thompson; Cathryn Tonne (2023). The 2023 report of the Lancet Countdown on health and climate change: the imperative for a health-centred response in a world facing irreversible harms. *The Lancet*, *402*(10419), 2346-2394. https://doi.org/10.1016/s0140-6736(23)01859-7 [Link]Farid Ullah Khan; Iftikhar Ahmad (2015). Review of Energy Harvesters Utilizing Bridge Vibrations. *Shock and Vibration*, *2016*, 1-21. https://doi.org/10.1155/2016/1340402 [Link]Moure, A.; Izquierdo Rodríguez, M.A.; Rueda, S. Hernández; Gonzalo, A.; Rubio-Marcos, F.; Cuadros, D. Urquiza; Pérez-Lepe, A.; Fernández, J.F. (2016). Feasible integration in asphalt of piezoelectric cymbals for vibration energy harvesting. *Energy Conversion and Management*, *112*, 246-253. https://doi.org/10.1016/j.enconman.2016.01.030 [Link]Rys, Dawid (2019). Consideration of dynamic loads in the determination of axle load spectra for pavement design. *Road Materials*

and Pavement Design, *22*(6), 1309-1328. https://doi.org/10.1080/14680629.2019.1687006 [Link]Wenjuan Sun; Guoyang Lu; Cheng Ye; Shiwu Chen; Yue Hou; Dawei Wang; Linbing Wang; Markus Oeser (2018). The State of the Art: Application of Green Technology in Sustainable Pavement. *Advances in Materials Science and Engineering*, *2018*(1). https://doi.org/10.1155/2018/9760464 [Link]Mogheisi, Meisam; Tavakoli, Hamid Reza; Peyghaleh, Elnaz (2023). Fragility Curve Development of Highway Bridges Using Probabilistic Evaluation (Case Study: Tehran City). https://doi.org/10.21203/rs.3.rs-2518429/v1 [Link]Wenjuan Sun; Guoyang Lu; Cheng Ye; Shiwu Chen; Yue Hou; Dawei Wang; Linbing Wang; Markus Oeser (2018). The State of the Art: Application of Green Technology in Sustainable Pavement. *Advances in Materials Science and Engineering*, *2018*(1). https://doi.org/10.1155/2018/9760464 [Link]John L. Wilkinson; Alistair B.A. Boxall; Dana W. Kolpin; Kmy Leung; Racliffe Weng Seng Lai; Cristóbal Galbán-Malagón; Aiko D. Adell; Julie Mondon; Marc Métian; Rob Marchant; Alejandra Bouzas-Monroy; Aida Cuní-Sanchez; Anja Coors; Pedro Carriquiriborde; Macarena Rojo; Christopher Gordon; Magdalena Cara; Monique Moermond; Thais Luarte; Vahagn Petrosyan; Yekaterina Perikhanyan; Clare S. Mahon; Christopher J. McGurk; Thilo Hofmann; Tapos Kormoker; Volga Iñiguez; Jessica Guzman-Otazo; Jean Leite Tavares; Francisco Gildasio De Figueiredo; María Tereza Pepe Razzolini; Victorien Dougnon; Gildas Gbaguidi; Oumar Traoré; Jules M. Blais; Linda E. Kimpe; Michelle Wong; Donald Wong; Romaric Ntchantcho; Jaime Pizarro; Guang-Guo Ying; Chang-Er Chen; Martha Isabel Páez-Melo; Jina Martínez-Lara; Jean-Paul Otamonga; John Poté; Suspense A. Ifo; Penelope Wilson; Silvia Echeverría-Sáenz; Nikolina Udiković-Kolić; Milena Milaković; Despo Fatta-Kassinos; Lida Ioannou-Ttofa; Vladimíra Belušová; Jan Vymazal; María Cárdenas-Bustamante; Bayable A. Kassa; Jeanne Garric; Arnaud Chaumot; Peter Gibba; Ilia Kunchulia; Sven Seidensticker; Gérasimos Lyberatos; Halldór Pálmar Halldórsson; Molly Melling; Shashidhar Thatikonda; Manisha Lamba; Anindrya Nastiti; Adee Supriatin; Nima Pourang; Ali Abedini; Omar Abdullah; Salem Gharbia; Francesco Pilla; Benny Chefetz; Tom Topaz; Koffi Marcellin Yao; Bakhyt Aubakirova; Raikhan Beisenova; Lydia Olaka; Jemimah K. Mulu; Peter Chatanga; Victor Ntuli; Nathaniel T. Blama; Sheck Sherif; Ahmad Zaharin Aris; Ley Juen Looi; Mahamoudane Niang; Seydou T. Traore; Rik Oldenkamp; Olatayo Michael Adetayo Ogunbanwo; Muhammad Ashfaq; Muhammad Iqbal; Ziad Abdeen; Aaron O'Dea; Jorge Manuel Morales-Saldaña; María Custodio; Heidi De la Cruz; Ian A. Navarrete; Fábio Carvalho; Alhaji Brima Gogra (2022). Pharmaceutical pollution of the world's rivers. *Proceedings of the National Academy of Sciences*, *119*(8). https://doi.org/10.1073/pnas.2113947119 [Link]Maina, James W.; Ozawa, Yoshiaki; Matsui, Kunihito (2012). Linear elastic analysis of pavement structure under non-circular loading. *Road Materials and Pavement Design*, *13*(3), 403-421. https://doi.org/10.1080/14680629.2012.705419 [Link]Daochun Li; Yining Wu; Andrea Da Ronch; Jinwu Xiang (2016). Energy harvesting by means of flow-induced vibrations on aerospace vehicles. *Progress in Aerospace Sciences*, *86*, 28-62. https://doi.org/10.1016/j.paerosci.2016.08.001 [Link]ZHAO, Hongduo; YU, Jian; LING, Jianming (2010). Finite element analysis of Cymbal piezoelectric transducers for harvesting energy from asphalt pavement. *Journal of the Ceramic Society of Japan*, *118*(1382), 909-915. https://doi.org/10.2109/jcersj2.118.909 [Link]Davino, D; Visone, C; Giustiniani, A (2012). Vibration energy harvesting devices based on magnetostrictive materials. *Bridge Maintenance, Safety and Management*, 1511-1518. https://doi.org/10.1201/b12352-217 [Link]Farid Ullah Khan; Iftikhar Ahmad (2015). Review of Energy Harvesters Utilizing Bridge Vibrations. *Shock and Vibration*, *2016*, 1-21. https://doi.org/10.1155/2016/1340402 [Link]Wenjuan Sun; Guoyang Lu; Cheng Ye; Shiwu Chen; Yue Hou; Dawei Wang; Linbing Wang; Markus Oeser (2018). The State of the Art: Application of Green Technology in Sustainable Pavement. *Advances in Materials Science and Engineering*, *2018*(1). https://doi.org/10.1155/2018/9760464 [Link]Chen, X.; Pan, Y.; Chen, J. (2010). Performance and Evaluation of a Fuel Cell–Thermoelectric Generator Hybrid System. *Fuel Cells*, *10*(6), 1164-1170. https://doi.org/10.1002/fuce.200900208 [Link]Lin, Teng; Pan, Yu; Chen, Shikui; Zuo, Lei (2018). Modeling and field testing of an electromagnetic energy harvester for rail tracks with anchorless mounting. *Applied Energy*, *213*, 219-226. https://doi.org/10.1016/j.apenergy.2018.01.032 [Link]Nasir, Diana SNM; Pantua, Conrad Allan Jay; Zhou, Bochao; Vital, Becky; Calautit, John; Hughes, Ben (2021). Numerical

analysis of an urban road pavement solar collector (U-RPSC) for heat island mitigation: Impact on the urban environment. *Renewable Energy*, *164*, 618-641. https://doi.org/10.1016/j.renene.2020.07.107 [Link]Pirisi, Andrea; Mussetta, Marco; Grimaccia, Francesco; Zich, Riccardo E. (2013). Novel Speed-Bump Design and Optimization for Energy Harvesting From Traffic. *IEEE Transactions on Intelligent Transportation Systems*, *14*(4), 1983-1991. https://doi.org/10.1109/tits.2013.2272650 [Link]El-hami, M.; Glynne-Jones, P.; White, N.M.; Hill, M.; Beeby, S.; James, E.; Brown, A.D.; Ross, J.N. (2001). Design and fabrication of a new vibration-based electromechanical power generator. *Sensors and Actuators A: Physical*, *92*(1-3), 335-342. https://doi.org/10.1016/s0924-4247(01)00569-6 [Link]Montoya, Arturo; Jagtap, Pranav; Papagiannakis, Athanassios; Dessouky, Samer; Walubita, Lubinda (2020). Numerical Study on Design and Installation of Energy-Harvesting Modules Embedded within a Flexible Pavement Structure. *Journal of Transportation Engineering, Part B: Pavements*, *146*(4). https://doi.org/10.1061/jpeodx.0000223 [Link]Duarte, Francisco; Ferreira, Adelino; Fael, Paulo (2018). Software Tool for Evaluation of Road Pavement Energy Harvesting Devices. *Advances in Intelligent Systems and Computing*, 107-121. https://doi.org/10.1007/978-3-319-77712-2_11 [Link]Rui Li; He Zhang; Li Wang; Guohua Liu (2021). A Contact-Mode Triboelectric Nanogenerator for Energy Harvesting from Marine Pipe Vibrations. *Sensors*, *21*(4), 1514-1514. https://doi.org/10.3390/s21041514 [Link]Zhang, Xitao (2025). MulVis: a visual analysis method for multilayer network Received:; Accepted: ; Published: date. https://doi.org/10.2139/ssrn.5996458 [Link]Claverie, Ezra (2024). Copyright Vigilantes. *Copyright Vigilantes*, 32-68. https://doi.org/10.14325/mississippi/9781496851338.003.0002 [Link]Marina Romanello; Claudia Di Napoli; Paul Drummond; Carole Green; Harry Kennard; Pete Lampard; Daniel Scamman; Nigel W. Arnell; Sonja Ayeb-Karlsson; Lea Berrang-Ford; Kristine Belesova; Kathryn Bowen; Wenjia Cai; Max Callaghan; Diarmid Campbell-Lendrum; Jonathan Chambers; Kim Robin van Daalen; Carole Dalin; Niheer Dasandi; Shouro Dasgupta; Michael Davies; Paula Domínguez-Salas; Robert Dubrow; Kristie L. Ebi; Matthew J. Eckelman; Paul Ekins; Luis E. Escobar; Lucien Georgeson; Hilary Graham; Samuel H Gunther; Ian Hamilton; Yun Hang; Risto Hänninen; Stella M. Hartinger; Kehan He; Jeremy Hess; Shih-Che Hsu; Slava Mikhaylov; Louis Jamart; Ollie Jay; Ilan Kelman; Gregor Kiesewetter; Patrick L. Kinney; Tord Kjellström; Dominic Kniveton; Jason Lee; Bruno Lemke; Yang Liu; Zhao Liu; Melissa Lott; Martín Lotto Batista; Rachel Lowe; Frances MacGuire; Maquins Odhiambo Sewe; Jaime Martínez-Urtaza; Mark Maslin; Lucy McAllister; Alice McGushin; Celia McMichael; Zhifu Mi; James Milner; Kelton Minor; Jan C. Minx; Nahid Mohajeri; Maziar Moradi-Lakeh; Karyn Morrissey; Simon Munzert; Kris A. Murray; Tara Neville; Maria Nilsson; Nick Obradovich; Megan B O'Hare; Tadj Oreszczyn; Matthias Otto; Fereidoon Owfi; Olivia Pearman; Mahnaz Rabbaniha; Elizabeth Robinson; Joacim Rocklöv; Renee N. Salas; Jan C. Semenza; Jodi D. Sherman; Liuhua Shi; Joy Shumake-Guillemot; Grant Silbert; Mikhail Sofiev; Marco Springmann; Jennifer Stowell; Meisam Tabatabaei; Jonathon Taylor; Joaquín Triñanes; Fabian Wagner; Paul Wilkinson; Matthew Winning; Marisol Yglesias-González; Shihui Zhang; Peng Gong; Hugh Montgomery; Anthony Costello (2022). The 2022 report of the Lancet Countdown on health and climate change: health at the mercy of fossil fuels. *The Lancet*, *400*(10363), 1619-1654. https://doi.org/10.1016/s0140-6736(22)01540-9 [Link]European Food Safety Authority (2022). The European Union One Health 2021 Zoonoses Report. *EFSA Journal*, *20*(12), e07666-e07666. https://doi.org/10.2903/j.efsa.2022.7666 [Link]Jusu M. Ngobeh; Mustapha Sannoh; Joseph Thullah (2023). A Comparative Analysis of the Sustainable Growth of Global Hydro, Solar, and Wind Power Systems (Renewable Energy Systems). *Open Journal of Energy Efficiency*, *12*(03), 49-61. https://doi.org/10.4236/ojee.2023.123005 [Link]